

Antitumor activity of nifurtimox is enhanced with tetrathiomolybdate in medulloblastoma

KAREN S. KOTO¹, PAMELA LESCAULT³, LAURENT BRARD⁴, KYUKWANG KIM⁴,
RAKESH K. SINGH⁴, JEFF BOND³, SHARON ILLENYE², MARNI A. SLAVIK²,
TAKAMARU ASHIKAGA^{1,5} and GISELLE L. SAULNIER SHOLLER^{1,2}

¹Vermont Cancer Center, Departments of ²Pediatrics, ³Microbiology and Molecular Genetics, University of Vermont College of Medicine, Burlington, VT; ⁴Department of Obstetrics and Gynecology, Women and Infants Hospital of RI, Alpert Medical School of Brown University, Providence, RI; ⁵Department of Medical Biostatistics, Vermont Cancer Center, University of Vermont, Burlington, VT, USA

Received November 22, 2010; Accepted January 17, 2011

DOI: 10.3892/ijo.2011.971

Abstract. Medulloblastoma, a neuroectodermal tumor arising in the cerebellum, is the most common brain tumor found in children. We recently showed that nifurtimox induces production of reactive oxygen species (ROS) and subsequent apoptosis in neuroblastoma cells both *in vitro* and *in vivo*. Tetrathiomolybdate (TM) has been shown to decrease cell proliferation by inhibition of superoxide dismutase-1 (SOD1). Since both nifurtimox and TM increase ROS levels in cells, we investigated whether the combination of nifurtimox and TM would act synergistically in medulloblastoma cell lines (D283, DAOY). Genome-wide transcriptional analysis, by hybridizing RNA isolated from nifurtimox and TM alone or in combination treated and control cells (D283) on Affymetrix exon array gene chips was carried out to further confirm synergy. We show that nifurtimox and TM alone and in combination decreased cell viability and increased ROS levels synergistically. Examination of cell morphology following drug treatment (nifurtimox + TM) and detection of caspase-3 activation via Western blotting indicated that cell death was primarily due to apoptosis. Microarray data from cells treated with nifurtimox and TM validated the induction of oxidative stress, as many Nrf2 target genes (HMOX1, GCLM, SLC7A11 and SRXN1) ($p < 10^{-5}$) were up-regulated. Other genes related to apoptosis, oxidative stress, DNA damage, protein folding and nucleosome formation were differentially involved in cells following treatment with nifurtimox + TM. Taken together, our results suggest nifurtimox and TM act synergistically in medulloblastoma cells *in vitro*, and that this combination warrants further studies as a new treatment for medulloblastoma.

Introduction

Medulloblastoma is the most common malignant brain tumor in children and accounts for 17% of all brain tumors in children 0-14 years old (1). Each year about five hundred children in the US are affected by the disease (2). Many of these children are less than 3 years old at diagnosis. These patients have a reduced 5-year survival rate or increased long-term morbidity. The overall 5-year survival rates range from 40 to 70%, with the lower rates corresponding to younger children. Current front-line treatments, which include intensive multiagent chemotherapy, surgical resection, and craniospinal radiation, often leave these patients with progressive neurocognitive and neuroendocrine defects (3-5). Despite these treatments, approximately one third of patients have recurrent disease. Therefore, novel, well-tolerated, effective treatments are needed to increase survival and prevent relapse without severe long-term toxicities.

Reactive oxygen species (ROS) are products of normal metabolism, and can also be induced by xenobiotic exposure. Depending on their concentration, ROS can lead to different outcomes for the cell because of their ability to modify many intracellular signaling pathways, as well as cause non-specific damage to DNA, lipids, and proteins (6). Oxidative stress activates the Nrf2 pathway, which activates a battery of genes involved in detoxification and prevention of free radical formation to protect the cell and facilitate cell survival (7). Under conditions of normal redox homeostasis, the cell maintains a balance between ROS generation or oxidative stress and antioxidant and repair defense mechanisms (8). At low levels, ROS can cause cell proliferation, while at high levels, ROS cause cytotoxicity, inhibition of cell proliferation, and induction of apoptosis (9). In order to upset this balance so that an overproduction of ROS leads to apoptosis, it is necessary to deliver an excess amount of ROS to cells (9). This is the strategy employed when utilizing exogenous ROS-generating drugs to treat tumor cells (10). In general, tumor cells are more active than normal cells in the production of O₂⁻ and are under intrinsic oxidative stress, which makes them rely more heavily on cellular antioxidant enzymes (11). Because

Correspondence to: Dr Giselle L. Saulnier Sholler, Department of Pediatrics, FAHC-Smith 559, 111 Colchester Ave., Burlington, VT 05401, USA
E-mail: gsholler@uvm.edu

Key words: medulloblastoma, nifurtimox, apoptosis, reactive oxygen species, tetrathiomolybdate

of this, tumor cells are more susceptible to excessive oxidative stress induced by xenobiotic or chemotherapeutic agents (9). Under excess oxidative stress due to chemotherapeutic agents, the normal cellular mechanisms that regulate ROS, including cellular antioxidant systems such as SOD, glutathione, thioredoxin, and sulfiredoxin, and repair mechanisms, are unable to maintain cellular redox homeostasis (9,11). The resulting overburden of ROS therefore leads to cell death (10).

One drug that generates the production of ROS is nifurtimox. Nifurtimox is a nitroheterocyclic compound that undergoes cellular reduction to nitro anion free radicals, hydrogen peroxide, and superoxide free radicals, which generate ROS (12-14). Originally nifurtimox was used to treat Chagas disease, which is caused by the parasite *Trypanosoma cruzi* (12). We previously reported a patient with neuroblastoma whose tumor appeared to respond to nifurtimox while undergoing conventional salvage chemotherapy (15). Subsequently we identified that nifurtimox causes ROS production, cytotoxicity and apoptosis of neuroblastoma cells in culture and in mouse xenograft models (16). Further, the *in vitro* cytotoxicity of nifurtimox in neuroblastoma cells is dependent on ROS generation (16). This led to a phase I clinical trial investigating the use of nifurtimox to treat pediatric patients with neuroblastoma where we determined the maximum tolerated dose (MTD) and its toxicity profile (76). Because nifurtimox is used to treat Chagas disease in the brain, it is known to cross the blood-brain barrier (12). It is readily absorbed after oral treatment with relatively low toxicity (17). As neuroblastoma and medulloblastoma are both tumors of the neuroectoderm, we hypothesized that nifurtimox might have the same cytotoxic effect on medulloblastoma cells as neuroblastoma cells.

Combining drugs that increase the level of ROS could potentially synergize the effects of nifurtimox on cell death. By increasing the amount of oxidative stress, the imbalance between the cellular oxidant species production and the antioxidant capability would be further increased. In combination with exogenous ROS-producing agents, drugs that reduce antioxidant capability could be used. Because of the increased oxidative stress in cancer cells, these cells are more vulnerable to antioxidant inhibition than normal cells (9). Deletion of the antioxidant gene superoxide dismutase-1 (SOD1) in *Trypanosoma brucei* has shown to increase sensitivity to nifurtimox (18). SOD1 is a copper/zinc enzyme found in the cytoplasm that converts superoxide into hydrogen peroxide and molecular oxygen, thereby maintaining low steady-state levels of superoxide (19-21). Deletion or inhibition of SOD1 results in an accumulation of superoxide in the cells (19-21). One way to inhibit SOD1 is by treatment with tetrathiomolybdate (TM), a copper chelator (22). By binding to copper, TM inhibits angiogenesis and SOD1 (23). TM is currently used to treat Wilson's disease and is a potent anti-angiogenic and anti-tumorigenic agent in mouse models. Based on these findings TM is being evaluated in human clinical oncology trials (22,24-28). In addition, high levels of SOD1 in tumors has been correlated with poor prognosis in medulloblastoma patients, making TM a good candidate for medulloblastoma treatment (29). By combining nifurtimox and TM to treat tumor cells, ROS are generated and antioxidant defense mechanisms are impaired, resulting in an accumulation of ROS. Our hypothesis is that this excess of ROS created by the nifurtimox and TM combination

treatment causes medulloblastoma cells to undergo apoptosis. A similar approach of combining an exogenous ROS-producing agent, arsenic trioxide, with a SOD1 inhibitor, 2-methoxyestradiol, has been shown to induce apoptosis of leukemia cells (30). TM has also been shown to cross the blood-brain barrier (31), making it a viable option for medulloblastoma treatment and reasonable to test it in combination with nifurtimox.

In our current study, we investigated the effects of nifurtimox treatment alone and in combination with TM on medulloblastoma cells. We found that nifurtimox and TM work synergistically to increase cellular levels of ROS and subsequent cell death in preclinical *in vitro* medulloblastoma cell lines. Induction of oxidative stress was further confirmed by gene expression profiles of medulloblastoma cells treated with nifurtimox and nifurtimox in combination with TM. These findings warrant further study to develop the combination of nifurtimox and TM as a potential treatment for medulloblastoma.

Materials and methods

Reagents. Nifurtimox (synthesized in the laboratory of Dr L. Brard, Women and Infants Hospital of RI/Brown University, Providence, RI) was dissolved in dimethyl sulfoxide (DMSO) as a 10 mg/ml stock and stored in aliquots at -20°C. TM (Sigma, St. Louis, MO) was dissolved in sterile water and stored in aliquots at -20°C. N-acetyl-L-cysteine (NAC) (Sigma, St. Louis, MO) was dissolved in RPMI (Mediatech) as an 800 mM stock and made fresh for each experiment.

Cell culture and treatment. The human medulloblastoma cell lines D283 (ATCC HTB-185) and DAOY (ATCC HTB-186) were maintained at 37°C in a 5% CO₂, humidified incubator in RPMI-1640 media (Mediatech) supplemented with 10% (v/v) fetal bovine serum (Gibco), 100 units/ml penicillin and 100 µg/ml streptomycin. Cells were grown to 75% confluency in 100 mm plates or T75 flasks. Cells were treated with nifurtimox (0, 10, 20 µg/ml) or TM (0, 1, 6.25 µg/ml) or the combination of 10 µg/ml nifurtimox and 6.25 µg/ml TM for 16-48 h for caspase activation studies.

Cell viability assay. Cell viability was measured with Calcein AM (Invitrogen, Carlsbad, CA). Calcein AM (a non-fluorescent molecule) is hydrolyzed by endogenous esterase into the highly negatively charged green fluorescent calcein. The fluorescent calcein is retained in the cytoplasm in live cells. Relative amount of Calcein AM directly corresponds to cell membrane integrity and cellular toxicity. The amount of dye transported into live cells over a fixed period of time was quantified by Calcein AM. D283 and DAOY cells (10,000 cells/well) were cultured in 48-well plates for 24 h and then treated with nifurtimox (10 µg/ml), TM (6.25 µg/ml) or the combination of nifurtimox (10 µg/ml) and TM (6.25 µg/ml) for 48 h. For the NAC studies, cells were pretreated with 10 mM NAC for 2 h, and nifurtimox (10 µg/ml), and TM (6.25 µg/ml) were subsequently added for the remaining 46-h of incubation. Vehicle-treated (0.1% DMSO or H₂O) cells were used as controls. After incubation, media was removed and fresh media without serum containing 2 µg/ml Calcein AM was added, then cells were incubated at 37°C for an additional

30 min. Fluorescence was measured at 520em/485ex using a BMG Fluostar microplate reader.

Isobologram statistical analysis. Statistical analysis of the cell survival data consisted of background correction, normalization and estimation of parameters reflecting the dependence of cell survival on drug concentration. More precisely, the fluorescence intensity, I , for each well was modeled using

$$I = \exp(\beta_{NfTx}^1 c_{NfTx} + \beta_{NfTx}^2 c_{NfTx}^2 + \beta_{TM}^1 c_{TM} + \beta_{TM}^2 c_{TM}^2 + \beta_{NfTx, TM}^2 c_{NfTx} c_{TM}) (N-B) + B + \varepsilon$$

where B is the mean intensity obtained from eight wells containing cell culture medium but no cells or drugs, N is the mean intensity obtained from four wells containing cells but no drugs, c_{drug} , $drug \in \{NfTx, TM\}$, is a drug concentration, and ε is a normally distributed error. Model parameters, $\beta_{drug(s)}^{order}$, $order \in \{1, 2\}$, were obtained using nonlinear parameter estimation.

Western blot analysis. Cells cultured in 100 mm plates were grown to 75% confluency and collected by scraping, re-suspended in E buffer (10 mM Tris pH 7.6, 50 mM NaCl, 5 mM EDTA, 50 mM NaF, 0.1 mM NaVO₄, 1% Triton, 10 µg/ml aprotinin, 10 µg/ml leupeptin, ABSF) and incubated on ice for 20 min to lyse the cells. Cell lysates were sonicated for 10 sec and centrifuged at 14,000 rpm for 20 min at 4°C. Protein concentration was determined with Bio-Rad protein assay (Bio-Rad, Hercules, CA). Cell lysates were electrophoresed on a 12% SDS-polyacrylamide gel and blotted onto polyvinylidene fluoride (PVDF) membrane, pore size 0.45 µm (Millipore). The blots were blocked with Aquablock (EastCoast Bio, New Berwick, ME) diluted 1:1 in PBS. The blots were probed with rabbit-derived antibody to cleaved caspase-3 and β-actin (Cell Signaling Technology, Beverly, MA). Protein bands were visualized using infrared dye-conjugated anti-rabbit secondary antibodies (LI-COR Biosciences, Lincoln, NE) and photographed using an Odyssey Infrared Imaging System (LI-COR Biosciences).

Measurement of ROS. Production of ROS was determined using dichlorodihydrofluorescein (DCF). Cells were pretreated with 25 µg/ml TM 24 h prior to nifurtimox (10 µg/ml) treatment. For nifurtimox treatment, media was changed to RPMI without phenol red and with glutamine and then nifurtimox was added to a final concentration of 10 µg/ml using minimal lighting. DMSO was added to the control cells. Cells were incubated in the dark at 37°C for 20-30 min. Carboxylated DCF (Invitrogen) (10 mM in DMSO and stored as a single use aliquot) was added to each foil protected flask to a final concentration of 20 µM. Cells were incubated in the dark at 37°C for 25-30 min. Cells were suspended in Accutase (Phoenix Flow, San Diego, CA) and incubated for 5 min at 37°C. Cells were centrifuged and re-suspended in 500 µl Accumax (Phoenix Flow) and 0.2% sodium azide. Fluorescence was measured by flow cytometry.

RNA extraction and microarray. D283 cells were treated with 10 µg/ml nifurtimox, 6.25 µg/ml TM, or the combination of 10 µg/ml nifurtimox and 6.25 µg/ml TM for 6 h. Samples were treated in duplicate. RNA extraction was done using the RNeasy micro kit (Qiagen, Valencia, CA) following the

manufacturer's instructions and eluted in Riboblock RNase inhibitor (Formentas). RIN's were >9. RNA (5 µg) was hybridized to each chip, and hybridization was performed using Affymetrix GeneChip Human Exon 1.0 ST arrays.

Oligonucleotide array analysis. Raw oligonucleotide array data includes a collection of images, one for each oligonucleotide probe for each chip. Each image is summarized in one probe intensity by the Vermont Genetics Network Microarray Facility using Affymetrix GCOS software. All other calculations were performed using R (32)/BioConductor (33,34) tools. Probe set sample matrix expression statistics were calculated using the Robust multichip average (RMA) method of Speed and co-workers (35,36), implemented in the aroma.affymetrix package of Bengtsson (37). Quality statistics were calculated using the simpleaffy (38) package. Differential expression statistics were analyzed in the context of annotation using Ingenuity Integrated Pathway Analysis. Sample groups are designated by C (control), N (nifurtimox alone), T (TM alone), or NT (nifurtimox and TM). Comparisons are designated by <Query Sample Group>m<Reference Sample Group> (m for minus). For each transcript cluster we tested the null hypotheses that there is no differential expression for each pair of sample groups, that there is no main effect of nifurtimox

$$\frac{NT + N - T - C}{2} = 0,$$

no main effect of TM

$$\frac{NT + T - N - C}{2} = 0,$$

or no nifurtimox-TM interaction

$$(NT - T) - (N - C) = 0.$$

Results

Nifurtimox and TM induce apoptosis of medulloblastoma cells in culture. The effect of nifurtimox and TM on the growth of D283 and DAOY medulloblastoma cells in culture was investigated. As shown in Fig. 1, single agent nifurtimox (A) and TM (B) inhibit the growth of both cell lines in a concentration-dependent manner. When treated with nifurtimox (5 µg/ml), cell viability of both D283 and DAOY cells were not affected, but treatment with nifurtimox (10 µg/ml) decreased cell viability to 70% in D283 cells and 44% in DAOY cells. Further, after 48-h exposure to 20 µg/ml nifurtimox, cell viability of D283 cells decreased to 23% and DAOY cells to 13% compared to vehicle-treated controls. Similarly, cell viability of D283 and DAOY cells was also decreased in a concentration-dependent manner upon increasing treatments of TM (Fig. 1B). When treated with 3.125 µg/ml TM, cell viability of D283 and DAOY decreased to 81 and 55% respectively. Upon treatment with 50 µg/ml TM for 48 h, cell viability of D283 and DAOY decreased to 35 and 59%, respectively. Based on these results, the nifurtimox concentration required to reach 50% inhibition of growth (GI₅₀) after 48-h treatment for these cell lines was estimated to be 8.4 µg/ml in D283 cells and 24.3 µg/ml in DAOY cells. Similarly, GI₅₀ for TM after 48-h treatment was estimated to be 22.3 µg/ml in D283 cells and 20.5 µg/ml in

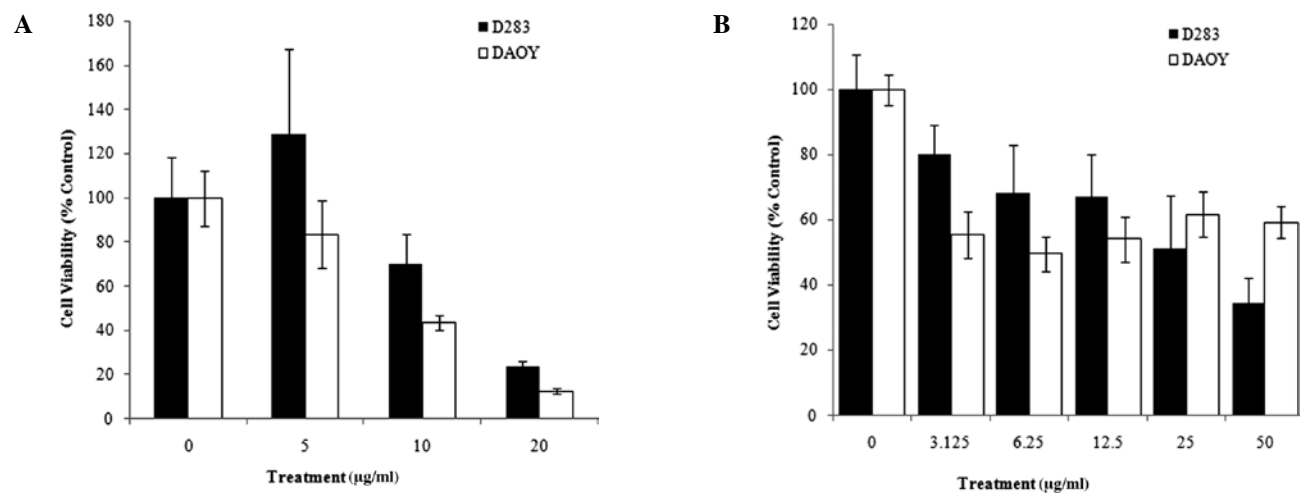


Figure 1. Nifurtimox and TM decrease medulloblastoma cell viability. D283 and DAOY medulloblastoma cells were incubated with increasing nifurtimox (A) and TM (B) concentrations in 48-well plates for 48 h. Cell viability was quantified using Calcein AM and expressed as percent of vehicle control.

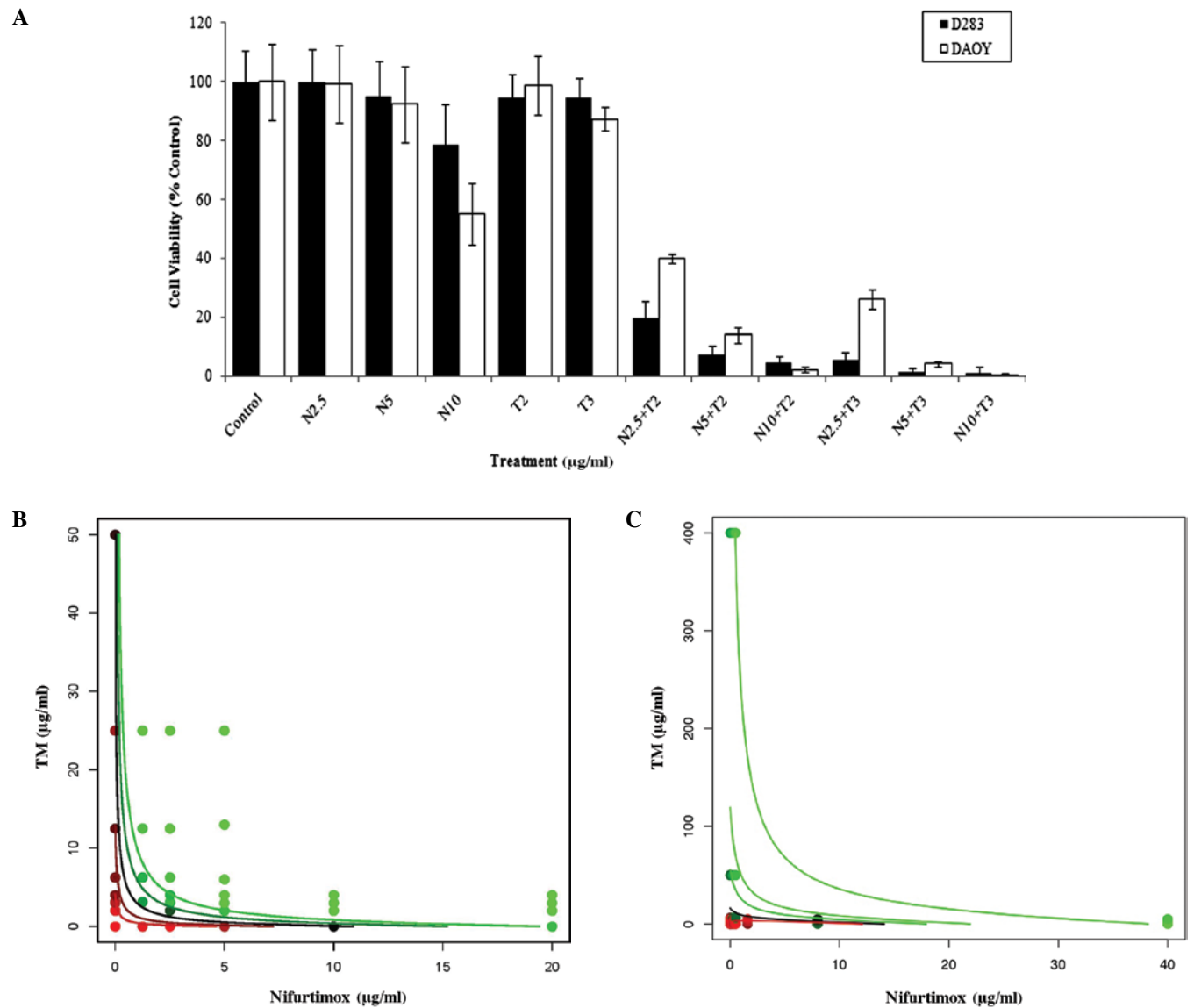


Figure 2. Nifurtimox and TM act synergistically to decrease medulloblastoma cell viability. (A), Combination of TM and nifurtimox at 48 h. Cells were treated with nifurtimox and TM as described. Cell viability was measured by Calcein AM assay. Viability is expressed as percentage control. Isobolograms show that the combination of TM and nifurtimox is synergistic for DAOY (B) and D283 (C) medulloblastoma cells. Points express mean survival after treatment with one or two drugs. Survival is expressed by the point's color, ranging from 100% survival (red) through 50% (black) to 0% (green). Contours represent the predictions obtained by fitting the model to data. Contour lines (90%, 75%, 50%, 25%, and 10% for DAOY; 90%, 50%, 10%, 1%, and 0.0000001% for D283) are colored according to the same scale as the points, that is, with a successful fit the lines will go through points of the same color.

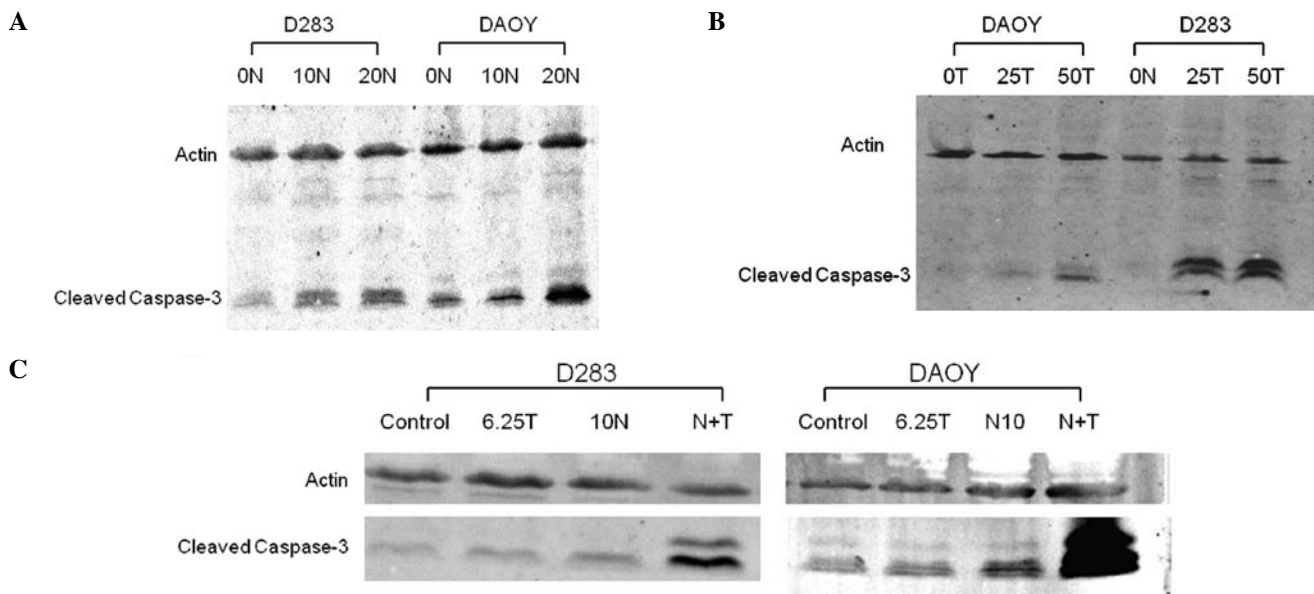


Figure 3. Nifurtimox induces apoptosis of medulloblastoma cells. Following nifurtimox (N), TM (T), or combination treatments (N+T), cells were lysed for Western blot analysis and probed for actin and cleaved caspase-3. (A), D283 and DAOY cells were incubated with 0, 10, or 20 $\mu\text{g/ml}$ nifurtimox for 16 h. (B), D283 and DAOY cells were treated with 0, 25, or 50 $\mu\text{g/ml}$ TM for 48 h. (C), D283 and DAOY cells were incubated with vehicle, 6.25 $\mu\text{g/ml}$ TM, 10 $\mu\text{g/ml}$ nifurtimox, or the combination for 16 h.

DAOY cells. In contrast, normal epithelial cells in culture exposed to nifurtimox do not experience these cytotoxic effects (15).

To determine if the combination of nifurtimox and TM has synergistic effects on cell viability, various concentrations of nifurtimox and TM were used to treat D283 and DAOY cells. As single agents, 2.5–5 $\mu\text{g/ml}$ nifurtimox and 2–3 $\mu\text{g/ml}$ TM did not alter cell viability at low doses (Fig. 2A). However, the combination of low doses of nifurtimox and TM greatly decreased cell viability (Fig. 2A). The addition of 1 $\mu\text{g/ml}$ TM decreased the GI_{50} of nifurtimox to 5.8 $\mu\text{g/ml}$ (40% decrease) in D283 and 1.2 $\mu\text{g/ml}$ (95% decrease) in DAOY cells. The combination of 2.5 $\mu\text{g/ml}$ nifurtimox with 2 $\mu\text{g/ml}$ TM decreased cell viability to 20 and 40% as compared to vehicle-treated D283 and DAOY cells, respectively. At 5 $\mu\text{g/ml}$ nifurtimox and 3 $\mu\text{g/ml}$ TM, the cell viability was further decreased to 1 and 4% as compared to vehicle-treated D283 and DAOY cells, respectively. Further, the efficacy of the combination of nifurtimox and TM in the treatment of medulloblastoma was analyzed by performing isobologram analysis of cell viability for DAOY (Fig. 2B) and D283 (Fig. 2C) cells. Fig. 2B and C show the isobologram data for the combination of nifurtimox and TM at varying concentrations. Parameter estimation strongly suggests drug synergism for both cell lines ($p < 10^{-80}$ and $p < 10^{-2}$ for DAOY and D283, respectively). Since the lines indeed go through points of the same color, with red lines going through red points and green lines going through green points, the model adequately describes the data.

Nifurtimox and TM in combination activate caspase-3 in medulloblastoma cells. To determine whether nifurtimox, TM and the combination of nifurtimox and TM decrease cell viability by inducing apoptosis, a Western blot analysis of lysates of drug-treated (single agent or in combination) vs. vehicle treated DAOY or D283 cells was performed to detect activated caspase-3, an initiator of the apoptotic cascade (39)

(Fig. 3). D283 and DAOY cells were exposed to 10 $\mu\text{g/ml}$ nifurtimox for 16 h, 6.25 $\mu\text{g/ml}$ TM for 48 h, and the combination of 10 $\mu\text{g/ml}$ nifurtimox and 6.25 $\mu\text{g/ml}$ TM for 16 h. Caspase activation was indicated by the concentration-dependent presence of cleaved caspase-3 when cells were treated with nifurtimox or TM alone. This caspase activation was not observed in vehicle-treated controls (Fig. 3A and B). When cells were treated with a combination of nifurtimox and TM, caspase-3 activation was increased as compared to vehicle-treated controls and cells treated with each of the drugs alone (Fig. 3C).

The combination of nifurtimox and TM increases ROS in medulloblastoma cells. To determine if nifurtimox and TM produce ROS in medulloblastoma cells, D283 and DAOY cells were pretreated with 25 $\mu\text{g/ml}$ TM for 24 h and then treated with 10 $\mu\text{g/ml}$ nifurtimox for 25–30 min. Cells were then incubated with carboxyl-DCF and fluorescence was measured by flow cytometry. Nifurtimox induced a 1.5-fold change in the DAOY cells and a 1.4-fold change in the D283 cells (Fig. 4A and B). TM induced a 1.5-fold change in the DAOY cells and a 1.3-fold change in the D283 cells (Fig. 4A and B). The combination of nifurtimox and TM induced a 3.1-fold change in the DAOY cells and a 1.6-fold change in the D283 cells, demonstrating increased levels of ROS in these cells (Fig. 4A and B).

To show that the cytotoxicity of nifurtimox was due to ROS, D283 and DAOY cells were pretreated with the antioxidant N-acetyl-L-cysteine (NAC) (10 mM) for 2 h and then treated with nifurtimox (10 $\mu\text{g/ml}$) or the combination of nifurtimox (10 $\mu\text{g/ml}$) and TM (6.25 $\mu\text{g/ml}$) for 48 h and cell viability was measured by Calcein AM assay. As shown in Fig. 4C, the viability of DAOY cells treated with NAC was the same as vehicle-treated cells, however, the viability of D283 cells was reduced (~20%) upon treatment with NAC (10 mM). Further, as shown previously (Fig. 2A), treatment with nifurtimox

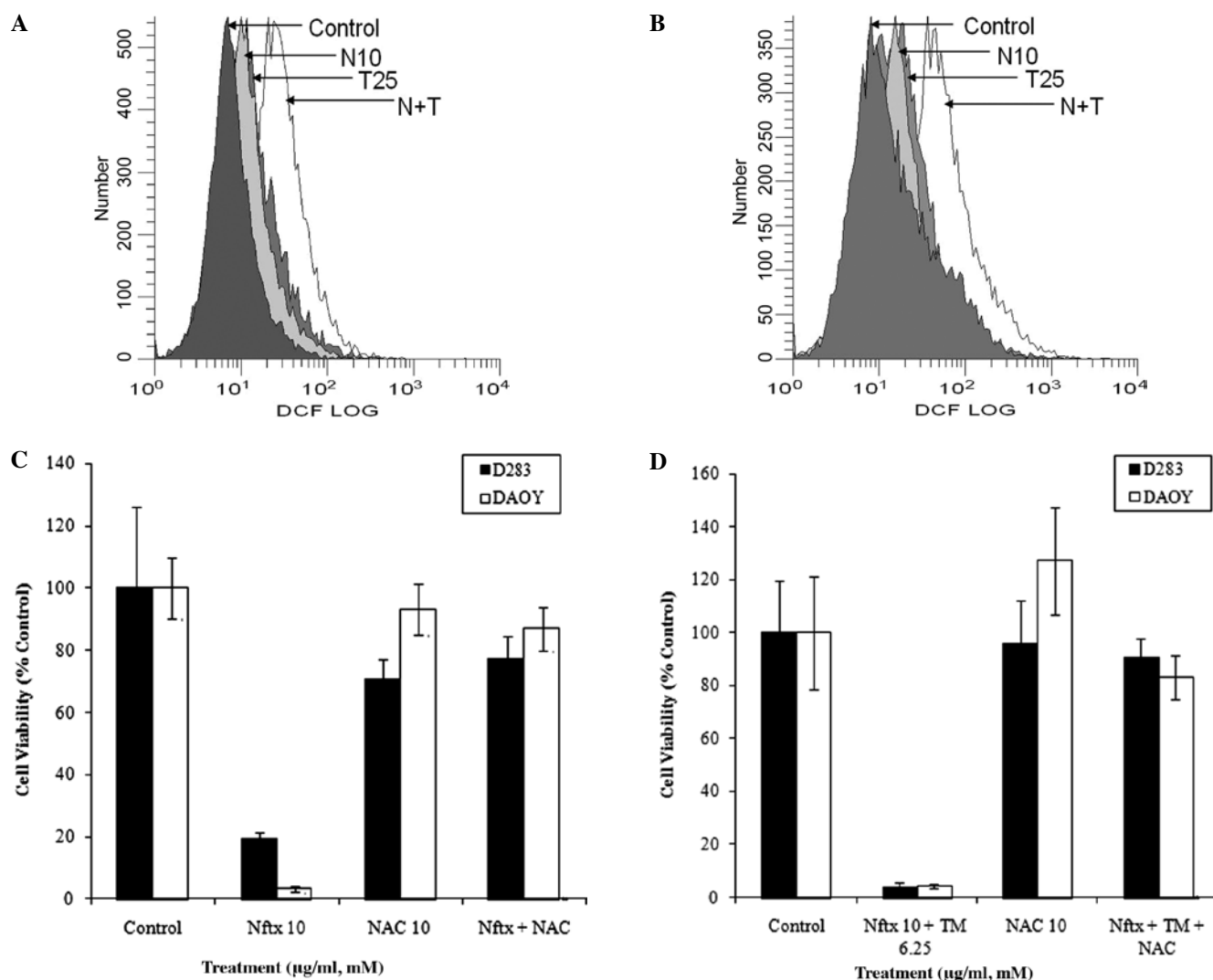


Figure 4. Nifurtimox induces formation of reactive oxygen species in medulloblastoma cells. (A and B), Cells were incubated with 10 $\mu\text{g/ml}$ nifurtimox (10-N), 25 $\mu\text{g/ml}$ TM (25-N), or the combination of 10 $\mu\text{g/ml}$ nifurtimox and 25 $\mu\text{g/ml}$ TM (N+T) for 25-30 min prior to treatment with carboxylated DCF. Cells were collected and analyzed by flow cytometry. (C), Cells were pre-incubated with 10 mM NAC for 2 h, then 10 $\mu\text{g/ml}$ nifurtimox or the combination of 10 $\mu\text{g/ml}$ nifurtimox and 6.25 $\mu\text{g/ml}$ TM was added. Cell viability was quantified after 48 h using Calcein AM.

or the combination of nifurtimox and TM decreased cell viability (Fig. 4D). When cells were pretreated with NAC (10 mM) followed by nifurtimox (10 $\mu\text{g/ml}$), or nifurtimox (10 $\mu\text{g/ml}$) and TM (6.25 $\mu\text{g/ml}$), cell viability of DAOY and D283 cells recovered to the same level of controls, confirming that ROS activation indeed mediates cytotoxicity induced by nifurtimox and the combination of nifurtimox and TM in these medulloblastoma cell lines (Fig. 4D).

Nifurtimox treatment resulted in activation of the Nrf2 pathway. To investigate changes in gene expression caused by treatments with nifurtimox, TM, or the combination of nifurtimox and TM, Affymetrix exon arrays were performed on RNA isolated from treated and control D283 cells. D283 cells were treated with DMSO vehicle, 10 $\mu\text{g/ml}$ nifurtimox, 6.25 $\mu\text{g/ml}$ TM, or the combination of 10 $\mu\text{g/ml}$ nifurtimox and 6.25 $\mu\text{g/ml}$ TM for 6 h, then RNA was isolated and exon arrays were performed.

Nrf2 target genes were non-randomly represented among genes judged differentially expressed. Genes differentially expressed in response to nifurtimox in either the absence

(NmC) or presence (NTmT) of TM were identified based on a p-value threshold of 0.05 (Fig. 5A and B). The nonrandom representation of Nrf2 pathway genes was significant at $p < 3 \times 10^{-6}$ and $p < 2 \times 10^{-6}$, respectively (Fig. 5A-D). The response of these genes to nifurtimox was very similar in NmC and NTmT (Fig. 5C), such that the nonrandom representation of Nrf2 pathway genes among genes identified as differentially expressed using the main effect of nifurtimox was significant at $p < 3 \times 10^{-8}$. Nrf2 pathway genes responding to nifurtimox with a greater than 2-fold change included HMOX1, GCLM, SLC7A11, and SRXN1, which were significant at $p < 10^{-5}$ in the NmC, NTmT and main effect comparisons (Fig. 5D). Ingenuity pathways analysis (IPA) was used to generate the NRF2 pathway, which has been overlaid with relative gene expression levels of the main effect of nifurtimox (Fig. 6). Other differentially expressed genes included those involved in apoptosis, response to oxidative stress, response to DNA damage, protein folding, and nucleosome formation (Table I).

The results of the other comparisons were less clear. The range of response to nifurtimox was < 3 -fold compared with 6-fold, and there was little correlation between TmC and

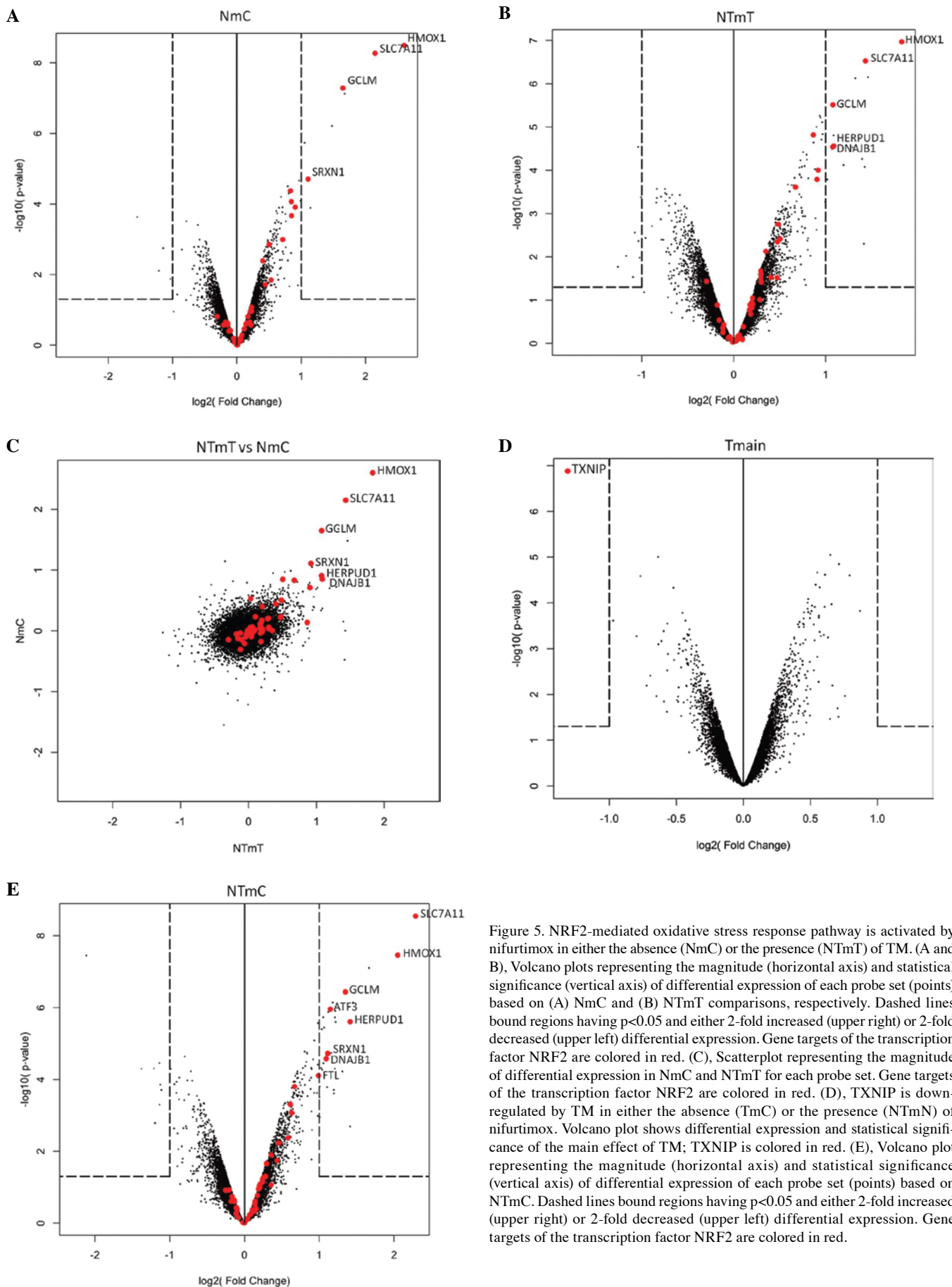


Figure 5. NRF2-mediated oxidative stress response pathway is activated by nifurtimox in either the absence (NmC) or the presence (NTmT) of TM. (A and B), Volcano plots representing the magnitude (horizontal axis) and statistical significance (vertical axis) of differential expression of each probe set (points) based on (A) NmC and (B) NTmT comparisons, respectively. Dashed lines bound regions having $p < 0.05$ and either 2-fold increased (upper right) or 2-fold decreased (upper left) differential expression. Gene targets of the transcription factor NRF2 are colored in red. (C), Scatterplot representing the magnitude of differential expression in NmC and NTmT for each probe set. Gene targets of the transcription factor NRF2 are colored in red. (D), TXNIP is down-regulated by TM in either the absence (TmC) or the presence (NTmN) of nifurtimox. Volcano plot shows differential expression and statistical significance of the main effect of TM; TXNIP is colored in red. (E), Volcano plot representing the magnitude (horizontal axis) and statistical significance (vertical axis) of differential expression of each probe set (points) based on NTmC. Dashed lines bound regions having $p < 0.05$ and either 2-fold increased (upper right) or 2-fold decreased (upper left) differential expression. Gene targets of the transcription factor NRF2 are colored in red.

NTmN. It may be that the time scale was too short to have seen a widespread response to TM that mediates the synergism

seen at 24-48 h. Nonetheless TXNIP was down-regulated in both comparisons and was associated with an adjusted p-value < 0.003 (Fig. 5D).

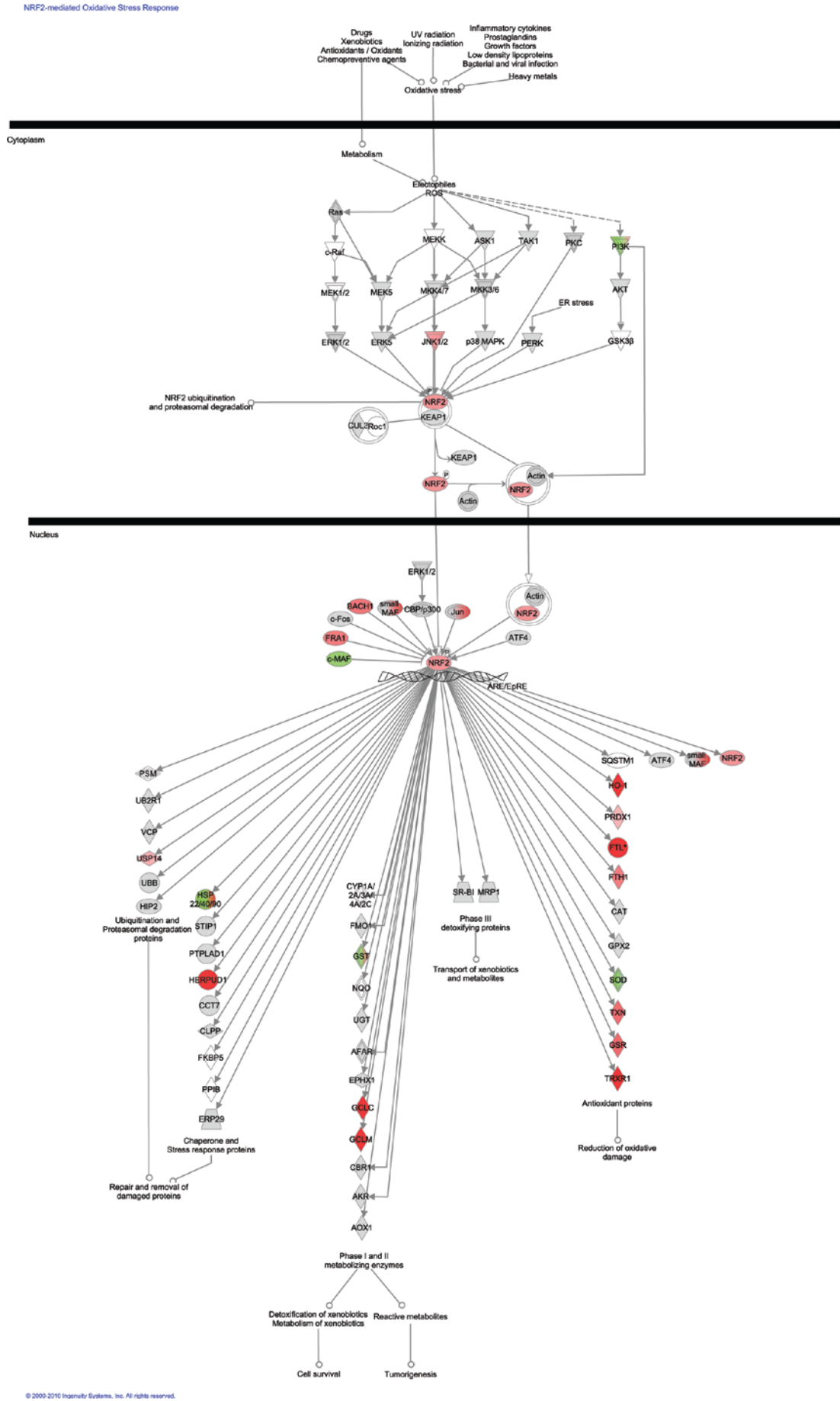


Figure 6. Canonical pathway analysis and differential expression induced by the main effect of nifurtimox. Data were analyzed through the use of Ingenuity Pathways Analysis (Ingenuity® Systems, www.ingenuity.com) and was used to generate the nuclear NRF2 pathway, which has been overlaid with relative gene expression levels of the main effect of nifurtimox. Red indicates up-regulation, and green indicates down-regulation.

Table I. Genes involved in apoptosis, oxidative stress, DNA damage, protein folding, or nucleosome structure that are differentially expressed in NmC, TmC, or NTmC.

Accession no.	Gene name	NmC f.c.	NmC p	TmC f.c.	TmC p	NTmC f.c.	NTmC p
Apoptosis							
NM_002061	Glutamate-cysteine ligase, modifier subunit (GCLM)	3.13	0.0003	1.21	0.9997	2.55	0.0115
NM_002133	Heme oxygenase (decycling) 1 (HMOX1)	6.07	5E-05	1.17	0.9997	4.14	0.00201
NM_006472	Thioredoxin interacting protein (TXNIP)	<u>1.49</u>	0.453	<u>2.11</u>	0.196	<u>4.34</u>	0.00022
NM_006186	Nuclear receptor subfamily 4 group A member 2 (NR4A2)	1.27	0.732	1.18	0.9997	2.27	0.00198
NM_004417	Dual specificity phosphatase 1 (DUSP1)	1.31	0.732	1.18	0.9997	2.31	0.00291
NM_019058	DNA-damage-inducible transcript 4 (DDIT4)	1.11	0.999	0.87	0.9997	2.29	0.0413
NM_004083	DNA-damage-inducible transcript 3 (DDIT3)	1.61	0.621	1.24	0.9997	2.48	0.0221
NM_015675	Growth arrest and DNA-damage-inducible, beta (GADD45B)	1.03	0.999	1.15	0.9997	2.09	0.00398
Oxidative stress/DNA damage/protein folding							
NM_002061	Glutamate-cysteine ligase, modifier subunit (GCLM)	3.13	0.0003	1.21	0.9997	2.55	0.00137
NM_080725	Sulfiredoxin 1 homolog (SRXN1)	2.16	0.0506	1.14	0.9997	2.16	0.0132
NM_002133	Heme oxygenase (decycling) 1 (HMOX1)	6.07	5E-05	1.17	0.9997	4.14	0.00022
NM_006472	Thioredoxin interacting protein (TXNIP)	<u>1.49</u>	0.453	<u>2.11</u>	0.196	<u>4.34</u>	0.00022
NM_001031716	Oligonucleotide/oligosaccharide-binding fold containing 2A (OBFC2A)	1.2	0.999	1.61	0.748	2.24	0.0132
NM_004417	Dual specificity phosphatase 1 (DUSP1)	1.31	0.732	1.18	0.9997	2.31	0.00291
NM_004083	DNA-damage-inducible transcript 3 (DDIT3)	1.61	0.621	1.24	0.9997	2.48	0.0221
NM_080725	Sulfiredoxin 1 homolog (<i>S. cerevisiae</i>) (SRXN1)	2.16	0.0506	1.14	0.9997	2.16	0.0132
NM_014685	Homocysteine/ER stress-inducible, ubiquitin-like domain member 1 (HERPUD1)	1.87	0.109	1.26	0.9997	2.66	0.00314
NM_001040619	Activating transcription factor 3 (ATF3)	1.1	0.999	1.22	0.9997	2.22	0.00245
NM_014331	Solute carrier family 7, member 11 (SLC7A11)	4.44	5E-05	1.81	0.21	4.89	5.3E-05
NM_006145	DnaJ (Hsp40) homolog, subfamily B, member 1 (DNAJB1)	1.8	0.149	1	0.9997	2.13	0.016
NM_012328	DnaJ (Hsp40) homolog, subfamily B, member 9 (DNAJB9)	1.47	0.284	1.05	0.9997	2.05	0.00414
NM_007034	DnaJ (Hsp40) homolog, subfamily B, member 4 (DNAJB4)	3.2	0.0004	1.27	0.9997	3.18	0.00037
Nucleosome formation							
NM_175055	Histone cluster 3, H2bb (HIST3H2BB)	<u>1.14</u>	0.999	<u>1.12</u>	0.9997	<u>2.308</u>	0.137
NM_003528	Histone cluster 2, H2be (HIST2H2BE)	<u>1.19</u>	0.999	<u>1.23</u>	0.9997	<u>2.208</u>	0.0186
NM_003522	Histone cluster 1, H2bf (HIST1H2BF)	<u>1.259</u>	0.931	<u>1.36</u>	0.9997	<u>2.1</u>	0.0132
NM_005322	Histone cluster 1, H1b (HIST1H1B)	<u>1.299</u>	0.999	<u>1.41</u>	0.9997	<u>2.28</u>	0.0372
NM_003519	Histone cluster 1, H2bl (HIST1H2BL)	<u>1.369</u>	0.668	<u>1.32</u>	0.9997	<u>2.01</u>	0.0143
NM_003521	Histone cluster 1, H2bm (HIST1H2BM)	<u>1.37</u>	0.982	<u>1.35</u>	0.9997	<u>2.75</u>	0.0242
NM_003544	Histone cluster 1, H4b (HIST1H4B)	<u>1.389</u>	0.891	<u>1.52</u>	0.9997	<u>2.18</u>	0.0345
NM_003513	Histone cluster 1, H2ab (HIST1H2AB)	<u>1.42</u>	0.822	<u>1.34</u>	0.9997	<u>2.31</u>	0.0211
NM_003537	Histone cluster 1, H3b (HIST1H3B)	<u>1.48</u>	0.856	<u>1.41</u>	0.9997	<u>2.57</u>	0.0251
NM_003511	Histone cluster 1, H2al (HIST1H2AL)	<u>1.81</u>	0.402	<u>1.53</u>	0.9997	<u>2.6</u>	0.0211
NM_005320	Histone cluster 1, H1d (HIST1H1D)	<u>2.04</u>	0.0727	<u>2.28</u>	0.196	<u>2.55</u>	0.00443

Table was constructed using GoTerms for apoptosis, oxidative stress, and response to DNA damage. Additional genes involved in these processes based on primary literature were added. Genes were chosen based on at least 2-fold change in one treatment, depicted in bold numbers. Treatment conditions include nifurtimox minus control (NmC), TM minus control (TmC), and nifurtimox and TM minus control (NTmC). Fold changes (f.c.) indicate sign fold changes, and p-values (p) represent adjusted p-values. Genes that are up-regulated are in black; genes that are down-regulated are underlined.

A subset of genes was differentially expressed in the NTmC as compared to NmC and TmC (Fig. 5E and Table I). Additional Nrf2 target genes, including HERPUD1, ATF3,

and DNAJB1, additional stress-inducible molecular chaperones including DNAJB9 and DNAJB4, and other genes involved in apoptosis and DNA damage including DUSP1, OBFC2A,

DDIT3, DDIT4, and GADD45B, were up-regulated by at least 2-fold change with adjusted p-values <0.05 (Fig. 5E and Table I). A large subset of histones were down-regulated by the nifurtimox and TM treatment, with adjusted p-values ranging from 0.004 to 0.136.

Discussion

Our study investigated whether the combination of nifurtimox and TM treatment would lead to an increase in ROS production and subsequent cell death in medulloblastoma cells. We found that nifurtimox and TM are cytotoxic to D283 and DAOY medulloblastoma cells in a concentration-dependent manner. When nifurtimox and TM are combined, cytotoxicity and ROS production are increased in these cell lines. Based on the isobologram data, nifurtimox and TM function synergistically. In support of the cell viability studies, the combination of nifurtimox and TM increases the amount of cleaved caspase-3 as compared to nifurtimox or TM alone, demonstrating that the loss in cell viability is due to synergistically enhanced apoptosis. The production of ROS causes the decrease in cell viability. As shown by DCF, nifurtimox and TM induce the production of ROS. When nifurtimox and TM are added in combination, the amount of ROS generated in medulloblastoma cells is greater than either treatment alone. Pretreatment of cells with NAC, an antioxidant, followed by treatment with nifurtimox or the combination of nifurtimox and TM, reverses the loss in cell viability. Therefore, the combination of nifurtimox and TM treatment functions synergistically to generate an excessive amount of ROS, which causes the medulloblastoma cells to undergo apoptosis leading to a decrease in cell viability.

Microarray data from medulloblastoma cells treated with nifurtimox and the combination of nifurtimox and TM confirms the mechanism of ROS generation. Adaptive oxidative stress response genes are induced in an effort to detoxify ROS, prevent free radical generation, and facilitate cell survival. The microarray analysis was performed six hours after treatment, so it represents an early cellular response. Several Nrf2 target genes, as well as other genes involved in apoptosis, DNA damage, oxidative stress, and protein folding, are induced by nifurtimox and nifurtimox plus TM combination treatment. These results are comparable to a study that investigated the *in vivo* gene expression of oxidative stress in mice treated with diquat, a redox cyler, and Sod1^{-/-} mice (40). Similar to our results in nifurtimox and TM treated medulloblastoma cells, up-regulation in several antioxidant genes, including Srxn1, Gclc, Txn2, and HMOX-1, in SOD1^{-/-} mice has been shown (40).

Specifically, nifurtimox and nifurtimox plus TM combination treatment causes up-regulation of several target genes of the Nrf2 pathway, regarded as the most important pathway in protecting cells against oxidative stress (41-45). Using Ingenuity software to analyze the microarray data in a nonrandom fashion, this pathway was regarded as the most highly involved pathway. Nrf2 is a basic leucine zipper transcription factor that binds to the antioxidant response element (ARE) in its target genes and regulates gene expression (42,46-52). Nrf2 target genes up-regulated at least 2-fold by nifurtimox and TM combination treatment include HMOX1, GCLM, SRXN1, HERPUD1, AFT3, DNAJB1, and SLC7A11. Some of these Nrf2 target genes are increased by nifurtimox treatment alone.

However, more Nrf2 target genes are up-regulated by nifurtimox plus TM combination treatment. For example, HMOX1 and GCLM expression increased in nifurtimox and nifurtimox plus TM treatment, but not TM treatment alone. These two genes were more up-regulated by nifurtimox alone (HMOX1 6.07-fold, GCLM 3.13-fold) than by nifurtimox plus TM combination treatment (HMOX1 3.55-fold, GCLM 2.11-fold), which may contribute to the decrease in cell survival seen in the combination treatment. Both HMOX1 and GCLM play important antioxidant roles in the cell. Up-regulation of these antioxidant genes that aid in cell survival signifies that the cells are under oxidative stress (7,8). HMOX1 is an antioxidant enzyme involved in the heme degradation process and confers resistance to stress-mediated cell injury (42,46,53). HMOX1 can also be induced by AP-1, NF- κ B, and their upstream kinases (ERK, JNK, p38MAPK, PI3K/Akt, PKC) (54). GCLM is the modulatory subunit of glutamate cysteine ligase, which catalyzes the first rate-limiting step of glutathione synthesis (55,56). GSH is the most abundant non-protein thiol in cell, and plays an essential role in the protection of cells against toxicants and metabolism of reactive compounds through reduction and conjugation reactions by reducing hydrogen peroxide and lipid hydroperoxides (8,57). Depletion of GSH by conjugation and reduction reactions results in an increased production of ROS (57). It is likely that nifurtimox and TM treatment depleted the GSH stores in the medulloblastoma cells. An increase in GSH levels serves as an adaptive response for the cell to defend itself against subsequent stresses.

In addition to the antioxidant genes HMOX1 and GCLM, two other antioxidant genes, SRXN1 and TXNIP, are regulated by nifurtimox, TM, and nifurtimox plus TM combination treatment. SRXN1 (sulfiredoxin 1) expression is up-regulated to the same levels with nifurtimox and combination treatment (2.16-fold), but unchanged with TM treatment. Recent studies have identified SRXN1 as a new Nrf2 target gene (58). Sulfiredoxin restores inactive peroxiredoxins (peroxidases) back to the thioredoxin cycle to prevent permanent oxidative inactivation of peroxiredoxins (58). In this way, sulfiredoxin and thioredoxin work in conjunction. The expression of TXNIP (thioredoxin-interacting protein) is repressed by nifurtimox (1.49-fold) and TM (2.11-fold) treatments alone, while the combination treatment (4.34-fold) showed a greater fold repression than either treatment alone. TXNIP inhibits the reducing activity of thioredoxin (TRX) through direct protein-protein interaction (59). Thioredoxin reduces ROS through reversible oxidation of thioredoxin at its two cysteine residues; thioredoxin is then reduced by thioredoxin reductase and NADPH (8). Therefore, when TXNIP gene is repressed, TRX expression is increased, leading to increased TRX-reducing activity, and potentially an improved cellular response to oxidative stress (60-63). While TRX is typically involved in inhibiting apoptosis, it can also regulate p53, which controls response of proapoptotic genes (63). It is possible that the synergistic down-regulation of TXNIP by the nifurtimox plus TM combination treatment contributes to the increase in apoptosis and decrease in cell survival. Clearly, both nifurtimox and nifurtimox plus TM combination treatment differentially regulate the expression of various antioxidant genes, which may affect the cellular response to oxidative damage and cell survival.

Additional Nrf2 target genes are up-regulated by nifurtimox and nifurtimox plus TM treatment, including SLC7A11, HERPUD1, and ATF3 (Table I). HERPUD1 expression is up-regulated in response to the accumulation of unfolded proteins in the endoplasmic reticulum (ER) as part of the ER stress response (64). SLC7A11 is a member of the heteromeric Na⁺-independent anionic amino acid transport system, where it exchanges cystine for glutamate, which ultimately enhances glutathione synthesis (65). Of these, SLC7A11 was up-regulated similarly by nifurtimox and nifurtimox plus TM treatment, while HERPUD1 and particularly ATF3 were more up-regulated by the nifurtimox plus TM combination treatment. ATF3, which is a bZIP-containing ATF/CREB family transcription factor, is a stress-responsive gene, as well as a p53 target gene with both protective and proapoptotic effects (66-71). Up-regulation of these Nrf2 target genes by the nifurtimox plus TM combination treatment may signify the increased oxidative stress caused by this treatment.

Microarray data also shows a change in gene expression of other genes involved in oxidative stress, DNA damage, apoptosis, protein folding, and nucleosome formation in cells treated with nifurtimox, TM, and the combination of nifurtimox and TM. Some of these genes are differentially regulated by nifurtimox or TM treatment alone, but all of them are significantly regulated at least 2-fold by the nifurtimox plus TM combination treatment (Table I). For example, NR4A2, an orphan nuclear receptor, is up-regulated 2.27-fold ($p=0.002$) by the combination treatment, but only 1.27-fold by nifurtimox and 1.18-fold by TM treatment. DUSP1 (also known as mkp-1) is the MAPK phosphatase-1, a nuclear phosphatase that dephosphorylates proteins of the MAPK family (p38 MAPK, JNK, ERK1/2) and thereby inactivates them, which may contribute to changes in cell cycle, cellular proliferation, and cell survival (72). The expression is slightly increased with nifurtimox (1.31-fold) or TM (1.18-fold) treatment alone, but is further increased in the combination treatment (2.31-fold). Typically DUSP1 expression is induced by oxidative stress and DNA damaging agents (72). OBFC2A (also known as hSSB2) showed similar expression pattern as DUSP1, slightly increased with nifurtimox (1.2-fold) or TM (1.61-fold) treatment alone, but increased more in the combination treatment (2.24-fold). While it is thought that this protein functions as a single-stranded DNA-binding protein to participate in the DNA damage response, the mechanism is unclear (73).

Three different DNA damage inducible genes, DDIT3, DDIT4, and GADD45B, showed the greatest level of expression in cells treated with the combination of nifurtimox and TM. This provides further evidence that DNA damage was likely induced, which could contribute to an increase in apoptosis. Furthermore, three stress-inducible molecular chaperones involved in protein folding, DNAJB1, DNAJB4, and DNAJB9, were increased by nifurtimox plus TM treatment. As molecular chaperones, these proteins bind to unfolded proteins or mutant proteins to ensure proper protein folding (74,75). Since oxidative stress causes the accumulation of damaged proteins, the up-regulation of these genes signifies a cytoprotective response to the proteotoxic stress induced by the nifurtimox plus TM treatment. Of potential interest is the down-regulation of several histones with the nifurtimox plus TM treatment. The histones HIST3H2BB, HIST1H2BF, HIST1H1B, HIST1H2BL,

HIST1H2BM, HIST1H2AB, HIST1H3B, HIST1H2AL, HIST1H1D were down-regulated by at least 2-fold with significant p-values of 0.004-0.04, with the exception of HIST3H2BB, which had a p-value of 0.14. The down-regulation of histone genes may affect nucleosome formation and cell replication. However, because of the complexity of histone gene clusters and the numerous copies of each histone gene, further validation of histone protein levels is necessary to confirm this result. The differential regulation of several genes involved in apoptosis, DNA damage, oxidative stress, protein folding, and nucleosome formation by the combination treatment further demonstrates the synergistic effect of nifurtimox and TM.

While it is clear from the cell viability data that nifurtimox and TM treatment are synergistic, the microarray data provide a genomic snapshot of this synergism. Certain target genes, including NR4A2, DUSP1, DDIT4, GADD45B, ATF3, DNAJB9, HIST3H2BB, and HIST2H2BE, appear to be differentially regulated in a synergistic manner by nifurtimox and TM combination treatment as compared to either treatment alone. Furthermore, it is obvious that the cells are responding to oxidative stress by turning on several different antioxidant genes, particularly targets of the Nrf2 pathway. Based on the data, the combination of nifurtimox and TM generates an overwhelming level of ROS which results in oxidative stress. It is possible that earlier or later time points than 6 h might provide more insight into the mechanism by which these two drugs function synergistically to decrease the viability by inducing apoptosis of medulloblastoma cells. Further experiments are underway to develop the combination of nifurtimox and TM as a potential treatment for medulloblastoma.

Acknowledgements

We thank Erika Currier for careful data analysis and Barton Kamen and Rae Nishi for critical reading of the manuscript. We also thank Scott Tighe of the Vermont Genetics Network. This publication was made possible by the Vermont Genetics Network through Grant no. P20 RR16462 from the INBRE Program of the National Center for Research Resources (NCRR), a component of the National Institutes of Health (NIH). Its contents are solely the responsibility of the authors and do not necessarily represent the official views of NCRR and NIH.

References

1. CBTRUS Supplement Report: Primary Brain Tumors in the United States. Central Brain Tumor Registry of the United States, Hinsdale, IL, 2004.
2. McNeil DE, Cote TR, Clegg L and Rorke LB: Incidence and trends in pediatric malignancies medulloblastoma/primitive neuroectodermal tumor: a SEER update. *Surveillance Epidemiology and End Results. Med Pediatr Oncol* 39: 190-194, 2002.
3. Grill J and Bhargava R: Recent developments in chemotherapy of paediatric brain tumors. *Curr Opin Oncol* 19: 612-615, 2007.
4. Mulhern RK, Palmer SL, Merchant TE, *et al*: Neurocognitive consequences of risk-adapted therapy for childhood medulloblastoma. *J Clin Oncol* 23: 5511-5519, 2005.
5. Ribi K, Rely C, Landolt MA, Alber FD, Boltshauser E and Grotzer MA: Outcome of medulloblastoma in children: long-term complications and quality of life. *Neuropediatrics* 36: 357-365, 2005.
6. Pan JS, Hong MZ and Ren JL: Reactive oxygen species: a double-edged sword in oncogenesis. *World J Gastroenterol* 15: 1702-1707, 2009.

7. Kaspar JW, Niture SK and Jaiswal AK: Nrf2:Keap1 signaling in oxidative stress. *Free Radic Biol Med* 47: 1304-1309, 2009.
8. Circu ML and Aw TY: Reactive oxygen species, cellular redox systems, and apoptosis. *Free Radic Biol Med* 48: 749-762, 2010.
9. Fang J, Seki T and Maeda H: Therapeutic strategies by modulating oxygen stress in cancer and inflammation. *Advanced Drug Deliv Rev* 61: 290-302, 2009.
10. Mates JM, Segura JA, Alonso FJ and Marquez J: Intracellular redox status and oxidative stress: implications for cell proliferation, apoptosis, and carcinogenesis. *Arch Toxicol* 82: 273-299, 2008.
11. Lau AT, Wang Y and Chiu JF: Reactive oxygen species: current knowledge and applications in cancer research and therapeutic. *J Cell Biochem* 104: 657-667, 2008.
12. Raether W and Hanel H: Nitroheterocyclic drugs with broad spectrum activity. *Parasitol Res* 90: 19-39, 2003.
13. Maya JD, Bollo S, Nunez-Vergara LJ, Squella JA, Repetto Y, Morello A, Perie J and Chauviere G: Trypanosoma cruzi: effect and mode of action of nitroimidazole and nitrofuran derivatives. *Biochem Pharmacol* 65: 999-1006, 2003.
14. Ramakrishna Rao DN and Mason RP: Generation of nitro radical anions of some 5-nitrofurans, 2- and 5-nitroimidazoles by norepinephrine, dopamine, and serotonin. *J Biol Chem* 262: 11731-11736, 1987.
15. Saulnier Sholler GL, Kalkunte S, Greenlaw C, McCarten K and Forman E: Antitumor activity of nifurtimox observed in a patient with neuroblastoma. *J Pediatr Hematol Oncol* 28: 693-695, 2006.
16. Saulnier Sholler GL, Brard L, Straub JA, Dorf L, Illenye S, Koto K, Kalkunte S, Bosenberg M, Ashikaga T and Nishi R: Nifurtimox induces apoptosis of neuroblastoma cells *in vitro* and *in vivo*. *J Pediatr Hematol Oncol* 31: 187-193, 2009.
17. Paulos C, Paredes J, Vasquez I, Thambo S, Arancibia A and Gonzalez-Martin G: Pharmacokinetics of a nitrofuran compound, nifurtimox, in healthy volunteers. *Int J Clin Pharmacol Ther Toxicol* 27: 454-457, 1989.
18. Prathalingham SR, Wilkinson SR, Horn D and Kelly JM: Deletion of the trypanosoma brucei superoxide dismutase gene *sodB1* increases sensitivity to nifurtimox and benznidazole. *Antimicrob Agents Chemother* 51: 755-758, 2007.
19. Fridovich I: Superoxide radical and superoxide dismutases. *Annu Rev Biochem* 64: 97-112, 1995.
20. Imlay JA and Fridovich I: Assay of metabolic superoxide production in *Escherichia coli*. *J Biol Chem* 266: 6957-6965, 1991.
21. Fridovich I: The biology of oxygen radicals. *Science* 201: 875-880, 1978.
22. Chidambaram MV, Barnes G and Frieden E: Inhibition of ceruloplasmin and other copper oxidases by thiomolybdate. *J Inorg Biochem* 22: 231-239, 1984.
23. Brewer GJ, Askari F, Dick RB, Sitterly J, Fink JK, Carlson M, Kluin KJ and Lorincz MT: Treatment of Wilson's disease with tetrathiomolybdate: V. control of free copper by tetrathiomolybdate and a comparison with trientine. *Translational Res* 154: 70-77, 2008.
24. Gartner EM, Griffith KA, Pan Q, Brewer GJ, Henja GF, Merajver SD and Zalupski MM: A pilot trial of the anti-angiogenic copper lowering agent tetrathiomolybdate in combination with irinotecan, 5-fluoracil, and leucovorin for metastatic colorectal cancer. *Invest New Drugs* 27: 159-165, 2009.
25. Redman BG, Esper P, Pan Q, Dunn RL, Hussain HK, Chenevert T, Brewer GJ and Merajver SD: Phase II trial of tetrathiomolybdate in patients with advanced kidney cancer. *Clin Cancer Res* 9: 1666-1672, 2003.
26. Brewer GJ, Dick RD, Grover DK, *et al*: Treatment of metastatic cancer with tetrathiomolybdate, an anticopper, antiangiogenic agent: phase I study. *Clin Cancer Res* 6: 1-10, 2006.
27. Lowndes SA, Adams A, Timms A, *et al*: Phase I study of copper-binding agent ATN-224 in patients with advanced solid tumors. *Clin Cancer Res* 14: 7526-7534, 2008.
28. Pass HI, Brewer GJ, Dick R, Carbone M and Merajver S: A phase II trial of tetrathiomolybdate after surgery for malignant mesothelioma: final results. *Ann Thorac Surg* 86: 383-390, 2008.
29. Kurisaka M and Mori K: Immunohistochemical study of medulloblastoma with a monoclonal antibody against human copper and zinc-superoxide dismutase. *Neurol Med Chir* 36: 220-223, 1996.
30. Hileman EO, Liu J, Albitar M, Keating MJ and Huang P: Intrinsic oxidative stress in cancer cells: a biochemical basis for therapeutic selectivity. *Cancer Chemother Pharmacol* 53: 209-219, 2004.
31. Dincer Z: Copper toxicity in sheep: studies on copper chelation by ammonium tetrathiomolybdate (TTM) and metallothionein. [dissertation]. University of Liverpool, Liverpool, 1994.
32. R Development Core Team. R: A Language and Environment for Statistical Computing. Available from: <http://www.R-project.org>, 2009.
33. Gentleman RC: Bioinformatics and computational biology solutions using R and Bioconductor, in statistics for biology and health. Springer Science & Business Media, New York, 2005.
34. Gentleman RC, Carey VJ, Bates DM, Bolstad B, Dettling M, Dudoit S, Ellis B, Gautier L, Ge Y, Gentry J, Hornik K, Hothorn T, Huber W, Iacus S, Irizarry R, Leisch F, Li C, Maechler M, Rossini AJ, Sawitzki G, Smith C, Smyth G, Tierney L, Yang JY and Zhang J: Bioconductor: open software development for computational biology and bioinformatics. *Genome Biol* 5: R80, 2004.
35. Irizarry RA, Bolstad BM, Collin F, Cope LM, Hobbs B and Speed TP: Summaries of Affymetrix GeneChip probe level data. *Nucleic Acids Res* 31: 5, 2003.
36. Bolstad BM, Irizarry RA, Astrand M and Speed TP: A comparison of normalization methods for high density oligonucleotide array data based on variance and bias. *Bioinformatics* 19: 185-193, 2003.
37. Bengtsson H, Simpson K, Bullard J and Hansen K: Aroma. Affymetrix: a generic framework in R for analyzing small to very large Affymetrix data sets in bounded memory, in Technical Report #745. Department of Statistics, University of California, Berkeley, 2008.
38. Wilson CL and Miller CJ: Simpleaffy: a BioConductor package for Affymetrix quality control and data analysis. *Bioinformatics* 21: 3683-3685, 2005.
39. Thornberry NA and Lazebnik Y: Caspases: enemies within. *Science* 281: 1312-1316, 1998.
40. Han ES, Muller FL, Perez VI, *et al*: The *in vivo* gene expression signature of oxidative stress. *Physiol Genom* 34: 112-126, 2008.
41. Jaiswal AK: Nrf2 signaling in coordinated activation of anti-oxidant gene expression. *Free Radic Biol Med* 36: 1199-1207, 2004.
42. Dhakshinamoorthy S, Long DJ and Jaiswal AK: Antioxidant regulation of genes encoding enzymes that detoxify xenobiotics and carcinogens. *Curr Top Cell Regul* 36: 201-206, 2000.
43. Zhang DD: Mechanistic studies of the Nrf2-Keap1 signaling pathway. *Drug Metab Rev* 38: 769-789, 2006.
44. Kobayashi M and Yamamoto M: Nrf2-Keap1 regulation of cellular defense mechanisms against electrophiles and reactive oxygen species. *Adv Enzyme Regul* 46: 113-140, 2006.
45. Copple IM, Goldring CE, Kitteringham NR and Park BK: The Nrf2-Keap1 defense pathway: role in protection against drug-induced toxicity. *Toxicology* 246: 24-33, 2008.
46. Jaiswal AK: Regulation of genes encoding NAD(P)H:quinone oxidoreductases. *Free Radic Biol Med* 29: 252-254, 2000.
47. Bloom D, Dhakshinamoorthy S, Wang W, Celli CM and Jaiswal AK: Role of NF-E2 related factors in oxidative stress. In: *Cell and Molecular Responses to Stress, Protein Adaptation and Signal Transduction*. Storey KB and Storey JM (eds). Elsevier, Amsterdam, pp229-238, 2001.
48. Venugopal R and Jaiswal AK: Nrf1 and Nrf2 positively and c-Fos and Fra1 negatively regulate the human antioxidant response element-mediated expression of NAD(P)H:quinone oxidoreductase1 gene. *Proc Natl Acad Sci USA* 93: 14960-14965, 1996.
49. Alam J, Stewart D, Touchard C, Boinapally S, Choi MK and Cook JL: Nrf2, a Cap'n/Collar transcription factor, regulates induction of the heme oxygenase-1 gene. *J Biol Chem* 274: 26071-26078, 1999.
50. Wild AC, Moinova HR and Mulcahy RT: Regulation of g-glutamylcysteine synthetase subunit gene expression by transcription factor Nrf2. *J Biol Chem* 274: 33627-33636, 1999.
51. Nguyen T, Huang HC and Pickett CB: Transcriptional regulation of the antioxidant gene response element: activation by Nrf2 and repression by MafK. *J Biol Chem* 275: 15466-15473, 2000.
52. Andrews NC, Erdjument-Bromage H, Davidson MB, Tempst P and Orkin SH: Erythroid transcription factor NF-E2 is a haematopoietic-specific basic leucine zipper protein. *Nature* 339: 722-727, 1993.
53. Tenhunen R, Marver MS and Schmid R: The enzymatic conversion of heme to bilirubin by microsomal heme oxygenase. *Proc Natl Acad Sci USA* 61: 748-755, 1968.
54. Prawn A, Kundu JK and Surh YJ: Molecular basis of heme oxygenase-1 induction: implications for chemoprevention and chemoprotection. *Antioxidants Redox Signaling* 7: 1688-1703, 2005.
55. Lu SC: Regulation of glutathione synthesis. *Molecular Aspects Medicine* 30: 42-59, 2009.

56. Krzywanski DM, Dickinson DA, Iles KE, Wigley AF, Franklin CC, Liu RM, Kavanagh TJ and Forman HJ: Variable regulation of glutamate cysteine ligase subunit proteins affects glutathione biosynthesis in response to oxidative stress. *Arch Biochem Biophys* 423: 116-125, 2004.
57. Soriano FX, Leveille F, Papadia S, Higgins LG, Varley J, Baxter P, Hayes JD and Hardingham GE: Induction of sulfiredoxin expression and reduction of peroxiredoxin hyperoxidation by the neuroprotective Nrf2 activator 3H-1,2-dithiole-3-thione. *J Neurochem* 107: 533-543, 2008.
58. Park JW, Mieyal JJ, Rhee SG and Chock PB: Deglutathionylation of 2-Cys peroxiredoxin is specifically catalyzed by sulfiredoxin. *J Biol Chem* 284: 23364-23374, 2009.
59. Nishiyama A, Matsui M, Iwata S, Hirota K, Masutani H, Nakamura H, Takagi Y, Sono H, Gon Y and Yodoi J: Identification of thioredoxin-binding protein-2/vitamin D(3) upregulated protein 1 as a negative regulator of thioredoxin function and expression. *J Biol Chem* 274: 21645-21650, 1999.
60. Patwari P, Higgins LJ, Chutkow WA, Yoshioka J and Lee RT: The interaction of thioredoxin with Txnip. Evidence for formation of a mixed disulfide by disulfide exchange. *J Biol Chem* 281: 21884-21891, 2006.
61. Junn E, Han SH, Im JY, Yang Y, Cho EW, Um HD, Kim DK, Lee KW, Han PL, Rhee SG and Choi I: Vitamin D3 upregulated protein 1 mediates oxidative stress via suppressing the thioredoxin function. *J Immunol* 164: 6287-6295, 2000.
62. Mitsui A, Hamuro J, Nakamura H, Kondo N, Hirabayashi Y, Ishizaki-Koizumi S, Hirakawa T, Inoue T and Yodoi J: Overexpression of human thioredoxin in transgenic mice controls oxidative stress and life span. *Antioxid Redox Signal* 4: 693-696, 2002.
63. Tonissen KF and Di Trapani G: Thioredoxin system inhibitors as mediators of apoptosis for cancer therapy. *Mol Nutr Food Res* 53: 87-103, 2009.
64. Hong SH, Kim J, Kim JM, Lee SY, Shin DS, Son KH, Han DC, Sung YK and Kwon BM: Apoptosis induction of 2'-hydroxycinnamaldehyde as a proteasome inhibitor is associated with ER stress and mitochondrial perturbation in cancer cells. *Biochem Pharmacol* 74: 557-565, 2007.
65. Lo M, Ling V, Wang YZ and Gout PW: The Xc-cystine/glutamate antiporter: a mediator of pancreatic cancer growth with a role in drug resistance. *Br J Cancer* 99: 464-472, 2008.
66. Kim KH, Jeong JY, Surh YJ and Kim KW: Expression of stress-response ATF3 is mediated by Nrf2 in astrocytes. *Nucleic Acids Res* 38: 48-59, 2010.
67. Turchi L, Aberdam I, Mazure N, Pouyssegur J, Deckert M, Kitajima S, Aberdam D and Viorolle T: Hif-2 α mediates UV-induced apoptosis through a novel ATF3-dependent death pathway. *Cell Death Differ* 15: 1472-1480, 2008.
68. Yoshida T, Sugiura H, Mitobe M, *et al*: ATF3 protects against renal ischemia-reperfusion injury. *J Am Soc Nephrol* 19: 217-224, 2008.
69. Lu D, Wolfgang CD and Hai T: Activating transcription factor 3, a stress-inducible gene, suppresses Ras-stimulated tumorigenesis. *J Biol Chem* 281: 10473-10481, 2006.
70. Nakagomi S, Suzuki Y, Namikawa K, Kiryu-Seo S and Kiyama H: Expression of the activating transcription factor 3 prevents c-Jun N-terminal kinase-induced neuronal death by promoting heat shock protein 27 expression and Akt activation. *J Neurosci* 23: 5187-5196, 2003.
71. Seijffers R, Mills CD and Woolf CJ: ATF3 increases the intrinsic growth rate of DRG neurons to enhance peripheral nerve regeneration. *J Neurosci* 27: 7911-7920, 2007.
72. Boutros T, Chevet E and Metrakos P: Mitogen-activated protein (MAP) kinase/MAP kinase phosphatase regulation: roles in cell growth, death, and cancer. *Pharmacol Rev* 60: 261-310, 2008.
73. Li Y, Bolderson E, Kumar R, Muniandy PA, Xue Y, Richard DJ, Seidman M, Pandita TK, Khanna KK and Wang W: hSSB1 and hSSB2 form similar multiprotein complexes that participate in DNA damage response. *J Biol Chem* 284: 23525-23531, 2009.
74. Ohtsuka K and Suzuki T: Roles of molecular chaperones in the nervous system. *Brain Res Bull* 53: 141-146, 2000.
75. Mitra A, Shevde LA and Samant RS: Multi-faceted role of HSP40 in cancer. *Clin Exp Metastasis* 26: 559-567, 2009.
76. Saulnier Sholler GL, Bergendahl GM, Brard L, Singh AP, Heath BW, Bingham PM, Ashikaga T, Kamen BA, Homans AC, Slavik MA, Lenox SR, Higgins TJ and Ferguson WS: A phase I study of nifurtimox in patients with relapsed/refractory neuroblastoma. *J Pediatr Hematol Oncol* 33: 25-30, 2011.